Frontoparietal Dysconnection in Covert Bipedal Activity for Enhancing the Performance of the Motor Preparation-Based Brain–Computer Interface

Chun-Ren Phang, *Graduate Student Member, IEEE*, Chia-Hsin Chen, Yuan-Yang Cheng, Yi-Jen Chen, and Li-Wei Ko, *Member, IEEE*

***Abstract*— Motor-based brain-computer interfaces (BCIs) were developed from the brain signals during motor imagery (MI), motor preparation (MP), and motor execution (ME). Motor-based BCIs provide an active rehabilitation scheme for post-stroke patients. However, BCI based solely on MP was rarely investigated. Since MP is the precedence phase before MI or ME, MP-BCI could potentially detect brain commands at an earlier state. This study proposes a bipedal MP-BCI system, which is actuated by the reduction in frontoparietal connectivity strength. Three substudies, including bipedal classification, neurofeedback, and post-stroke analysis, were performed to validate the performance of our proposed model. In bipedal classification, functional connectivity was extracted by Pearson's correlation model from electroencephalogram (EEG) signals recorded while the subjects were performing MP and MI. The binary classification of MP achieved short-lived peak accuracy of 73.73(±7.99)% around 200-400 ms post-cue. The peak accuracy was found synchronized to the MP-related potential and the decrement in frontoparietal connection strength. The connection strengths of the right frontal and left parietal lobes in the alpha range were found negatively correlated to the classification accuracy. In the subjective neurofeedback study, the majority of subjects reported that motor preparation instead of the motor imagery activated the frontoparietal dysconnection. Post-stroke study also showed that patients exhibit lower frontoparietal connections compared to healthy subjects during both MP and ME phases. These findings suggest that MP reduced alpha band functional frontoparietal connectivity and the EEG signatures of left and right foot MP could be discriminated more effectively during this phase. A neurofeedback paradigm based on the frontoparietal network could also be utilized to evaluate post-stroke rehabilitation training.**

***Index Terms*— Brain–computer interface, functional connectivity, motor preparation, motor imagery, neurorehabilitation.**

Manuscript received 6 April 2022; revised 25 July 2022 and 14 September 2022; accepted 6 October 2022. Date of publication 31 October 2022; date of current version 30 January 2023. This work was supported in part by the Ministry of Science and Technology (MOST) under Grant 111-2221-E-A49-167 and Grant 111-2823-8-A49-004, in part by the Center for Intelligent Drug Systems and Smart Bio-Devices (IDS^{2}B) from the Featured Areas Research Center Program within the framework of the Higher Education Sprout Project of the National Yang Ming Chiao Tung University and Ministry of Education (MOE) in Taiwan, in part by the National Yang Ming Chiao Tung University (NYCU)-Kaohsiung Medical University (KMU) Joint Research Project under Grant NYCU-KMU-111-I007, and in part by the Veterans General Hospitals and University of System Taiwan Joint Research Program under Grant VGHUST111-G6-1-1. *(Corresponding author: Li-Wei Ko.)*

This work involved human subjects or animals in its research. Approval of all ethical and experimental procedures and protocols was granted by the Institutional Review Board (IRB) of National Yang Ming Chiao Tung University under Case No.NYCU-REC-110-011E.

Chun-Ren Phang is with the International Ph.D. Program in Interdisciplinary Neuroscience (UST), Center for Intelligent Drug Systems and Smart Bio-Devices (IDS^{2}B), College of Biological Science and Technology, National Yang Ming Chiao Tung University, Hsinchu 30010, Taiwan.

Chia-Hsin Chen is with the College of Medicine, Kaohsiung Medical University, Kaohsiung 807, Taiwan, and also with the Department of Physical Medicine and Rehabilitation, and Regenerative Medicine and Cell Therapy Research Center, Kaohsiung Medical University, Kaohsiung 807, Taiwan.

Yuan-Yang Cheng is with the Department of Physical Medicine and Rehabilitation, Taichung Veterans General Hospital, Taichung 40705, Taiwan, also with the Department of Post-Baccalaureate Medicine, College of Medicine, National Chung Hsing University, Taichung 402, Taiwan, and also with the School of Medicine, National Yang Ming Chiao Tung University, Taipei 112, Taiwan.

Yi-Jen Chen is with the Department of Rehabilitation, Kaohsiung Municipal Siaogang Hospital, Kaohsiung 812, Taiwan, and also with the Department of Physical Medicine and Rehabilitation, and Regenerative Medicine and Cell Therapy Research Center, Kaohsiung Medical University, Kaohsiung 807, Taiwan.

Li-Wei Ko is with the International Ph.D. Program in Interdisciplinary Neuroscience (UST), Center for Intelligent Drug Systems and Smart Bio-Devices (IDS^{2}B), Department of Biological Science and Technology, College of Biological Science and Technology, Institute of Electrical and Control Engineering, National Yang Ming Chiao Tung University, Hsinchu 30010, Taiwan, and also with the Drug Development and Value Creation Research Center, the Department of Biomedical Science and Environment Biology, Kaohsiung Medical University, Kaohsiung 807, Taiwan (e-mail: lwko@nycu.edu.tw).

Digital Object Identifier 10.1109/TNSRE.2022.3217298

I. Introduction

BRAIN-COMPUTER interfaces (BCIs) are an emerging technology that allows users to communicate with external devices such as computers and exoskeletons by modulating their brain activity. Major efforts have focused on the development of BCIs. Numerous research have showed the possibility of computer-embedded devices such as robot [1], cursor [2], exoskeleton [3], wheelchair [4] and speller [5] to be controlled

This work is licensed under a Creative Commons Attribution-NonCommercial-NoDerivatives 4.0 License.
For more information, see https://creativecommons.org/licenses/by-nc-nd/4.0/

using electroencephalogram (EEG) signals. Steady-state visual evoked potential (SSVEP) and P300 evoked potential are exogenous BCI control signals, which require users to gaze at external stimuli such as flickering frequency or flashing letters to generate specific brainwaves [6], [7]. SSVEP and P300 BCI systems require little training time compared to MI-BCI. However, SSVEP and visual-based P300 require visual stimulus and tend to fail to generalize to patients suffering from uncontrolled eye movement [8]. On the other hand, an endogenous BCI system based on motor imagery (MI) sensorimotor rhythms requires no exogenous stimulus [9]. In the development of MI-BCI, users have to be trained to produce overt imagery movement of body parts such as arm, foot, or tongue [10], [11]. However, the performance of lower limb MI remains low because the motor cortex areas responsible for the activity in each foot are anatomically close to each other [12]. Studies based on functional magnetic resonance imaging [13], functional near-infrared spectroscopy [14], and EEG band power [15] found no significant difference between foot MI. Recent research attempted to classify lower limb motor activity based on the beta rebound and reported an average accuracy of 69.3% [16].

Functional connectivity estimated from macro-scale brain areas has been extensively studied to characterize various neurological disorders, such as schizophrenia [17], epilepsy [18], [19], Parkinson's disease [20], [21], Alzheimer's disease [22], mood disorders [23], [24] and attention deficit hyperactivity disorder [25]. A recent review [26] has discussed the applications of EEG-based functional connectivity and effective connectivity computed by Pearson's correlation, magnitude squared coherence, phase-locking value, transfer entropy, multivariate autoregression, directed transfer function, and partial directed coherence in the domain of upper limb MI-BCI. Moreover, given the fact that the cortices of the lower limb are anatomically close to each other [12], functional connectivity derived from EEG has shown superiority in distinguishing both upper and lower limb MIs compared to localized features such as common spatial pattern and band power [27], [28].

Despite major advancements in BCI research, around 15-30% of the population underperformed in producing neural signals to operate BCI systems [29], [30]. Recent studies have identified the inter-subject functional frontoparietal connectivity markers that contribute to the upper limb MI-BCI performance [31], [32]. However, the intra-subject mechanism of imagery that contributes to the enhanced MI-BCI performance was not investigated. These frontoparietal connections could potentially act as a BCI actuator, to filter the BCI commands estimated as low performing. Besides that, motor activities are mainly comprised of two modes, which are covert motor preparation (MP) or covert imagery of motor execution (MI) and overt motor execution (ME). Conventional MI-BCIs rarely independently evaluate the performance of MP or MI. In most cases, the performance was evaluated from time-series EEG signals which span both MP and MI. These indiscriminate paradigms were unable to pinpoint the exact mechanisms for high-performing motor-based BCI. Although several efforts have attempted to classify upper limb MP prior to both ME and MI [33], [34], the classification performances of MP and ME/MI were not simultaneously compared. The classification of MP would allow a more natural and instant control as brain commands could be detected in the early phase. Hence, we demonstrate the feasibility of a frontoparietal-connectivity-actuated lower limb MP-BCI system, using a wearable wireless EEG system. We also showed that this system could provide a new method of neurorehabilitation based on functional frontoparietal connectivity, to monitor the recovery outcome of rehabilitation therapy in real time.

The main novelty of this study is the implementation of a frontoparietal-connectivity-actuated lower limb MP-BCI system. Previous literature on connectivity methods has not investigated how the functional frontoparietal connectivities correlate to the bipedal classification performance during MP and MI phases. This study is an extension of our previous study. In [28], we successfully classified the functional connectivities of healthy individuals in 1-second bipedal motor imagery tasks with promising accuracy. Hence, in this current study, we further evaluate the distinguishability of functional connectivities during bipedal MP and MI tasks. The main objectives of this study are (1) To demonstrate the system design of the frontoparietal-actuated lower limb MP-BCI system; (2) To compare the classification performance of lower limb MP and MI; (3) To understand the subjective motor experience corresponds to frontoparietal functional connectivities; (4) To propose the application of the system for post-stroke lower limb rehabilitation.

II. Connectivity-Based MP-BCI System

A frontoparietal-connectivity-actuated lower limb MP-BCI system was proposed. The main components of the system included a wearable EEG device, functional connectivity analysis algorithm, and machine learning classifier. Users were embedded with a wireless EEG device for real-time EEG signal recording. The recorded signals were transmitted to a signal processing computer through Bluetooth. Functional frontoparietal connections were extracted to estimate the performance of MP-BCI commands. Simultaneously, brain-wide functional connectivity was computed from the EEG signals for the detection of left or right foot MP. The low-performing commands (brain-wide connectivity features) were filtered, to improve the general usability of the MP-BCI system. The system design was visualized in figure 1. The frontoparietal actuator developed in this study could also be used as a neurofeedback post-stroke rehabilitation paradigm.

A. Wearable EEG Device

The wearable EEG device used in the proposed MP-BCI system was St. EEG^{TM} Vega manufactured by Artise Biomedical Co., Ltd [35], Taiwan. This system was previously used in [36] to study the EEG activity of human attention. St. EEG^{TM} Vega consisted of a detachable amplifier, where signals were transmitted wirelessly through Bluetooth. It came with 35 water-based sponge sensors, including 32 recording electrodes located according to the international 10/20 placement, A1 and A2 reference electrodes, and FPz ground electrode. The recording electrodes encompassed FP1, FP2,

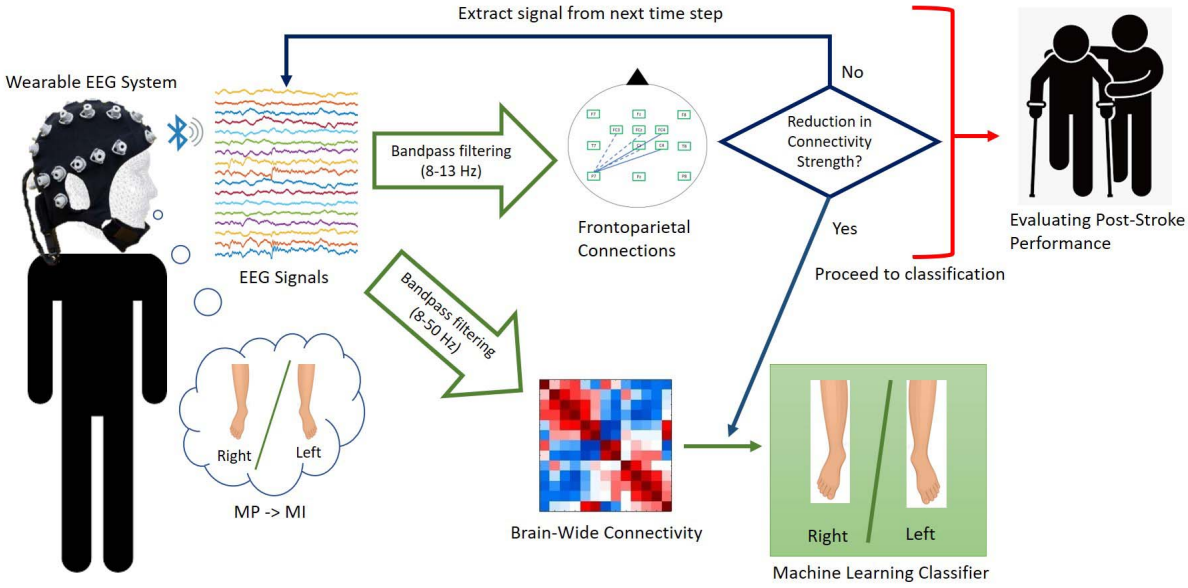

Fig. 1. The system design of frontoparietal-connectivity-actuated lower limb MP-BCI system, which includes a wearable EEG device connected to a computer via Bluetooth, functional connectivity analysis algorithm for the computation of brain-wide and frontoparietal networks, and machine learning classifier for the discrimination of left and right foot MP. The frontoparietal connectivity model could be used in post-stroke rehabilitation to monitor neural activity and provide a neurofeedback training paradigm (red lines).

AF3, AF4, F7, F3, Fz, F4, F8, FT7, FC3, FCz, FC4, FT8, T7, C3, Cz, C4, T8, TP7, CP3, CPz, CP4, TP8, P7, P3, Pz, P4, P8, O1, Oz, and O2. The detachable water-based sensors promote both the practicality and comfortability of the wearable EEG system. EEG signals were recorded using the device-accompanied Cynus data acquisition software with a sampling rate of 500 Hz. The recorded EEG signals were transferred via Bluetooth to a computer for the extraction of functional connectivity.

B. Functional Connectivity Analysis

Functional connectivity features were extracted from N-channel EEG epochs ($N = 32$) when subjects perform MP. The bivariate functional connectivity was extracted using Pearson's correlation from signals in all pairs of EEG electrodes. The computed correlation coefficients $r_{xy} \in [-1, 1]$ represent the weighted but undirected connectivity between brain regions. Based on this estimation, the connection strength is proportionate to the synchronization of voltage fluctuation between two recorded EEG signals, x and y. Pearson's correlation is the division of the covariance of signals x and y by the product of their standard deviations, as shown in Eq. 1. Weighted connections carry more information compared to unweighted connections, which could allow the machine learning classifier to learn from more informative features.

$$r_{xy} = \frac{\sum_{i=1}^{T}(x_i - \bar{x})(y_i - \bar{y})}{\sqrt{\sum_{i=1}^{T}(x_i - \bar{x})^2}\sqrt{\sum_{i=1}^{T}(y_i - \bar{y})^2}} \quad (1)$$

where $\bar{x}$ and $\bar{y}$ are the mean amplitude of signal x and y, while T is the length of time series. Positive correlation $r_{xy} > 0$ indicates that the amplitude of both signals are synchronized; while the amplitude of x and y are inverted in negative correlation $r_{xy} < 0$. The assembly of pairwise correlation from each pair of EEG signals produce a $N \times N$ symmetric connectivity matrix, R, which each element of the matrix represents the connectivity strength between two spatially distinct brain regions. To preserve the spatially proximal and weak connections, no additional preprocessing and thresholding were performed on the extracted functional connectivities. Since the MP/MI tasks were conducted with random stratification, the spurious connections would be present during both left and right foot tasks. These inherent spurious connections would not likely to pass statistical tests and affect the classification performance. The extracted brain-wide connectivity was used to train the machine learning classifier to distinguish left or right foot MP. Besides that, frontoparietal connections were extracted for the development of actuator to evaluate BCI performance.

C. Frontoparietal Connections and Classifier

The five frontoparietal connections (P7-C4, P7-Cz, P7-FC4, P7-FCz, P7-FC3) were by referring to [32], where the reduction in functional frontoparietal connectivity strength hinted at the commencement of motor-related BCI commands. The brain-wide connectivity estimated from temporal EEG signals with reduced frontoparietal connections would proceed to the classification step. A linear support vector machine (SVM) was shown to be able to classify connectivity features generated from lower limb MI with promising accuracy [28]. Hence, the machine learning classifier used in this system was linear SVM. SVM could maximize the distance between separating hyperplane and support vectors [37], in order to classify features extracted from different classes. SVM is a widely used machine learning algorithm because of its efficiency in solving classification problems. The diagonal (self-correlation, D) and

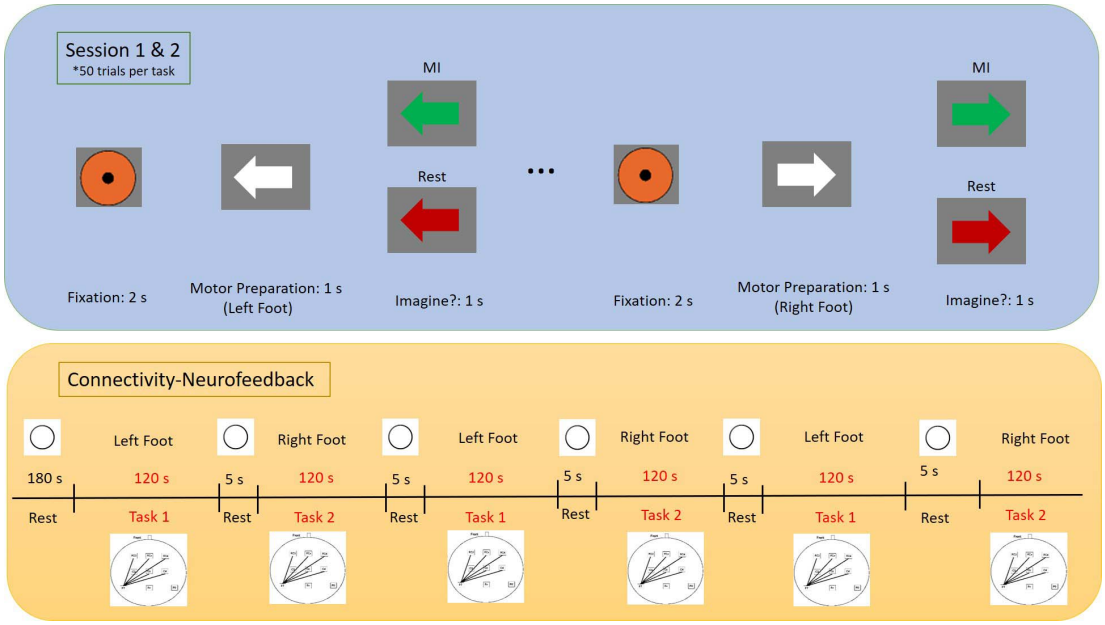

Fig. 2. Two data acquisition schemes were conducted in this study. The first experimental scheme (blue) was conducted for two sessions, where left or right arrows were prompted on a screen to cue the subjects to perform respective lower limb MP and MI. The second experimental scheme was a connectivity-based neurofeedback paradigm to investigate the relationship between subjective experience and neural activity during lower limb MP/MI.

the same connections in the symmetrical $N \times N$ connectivity matrices were removed, generating a feature dimension of $1/2 \times (N \times N - D)$. The EEG signals were recorded with 32 electrodes in this study, and the number of features fed into the classifier was 496. The output of the SVM classifier was binary $(-1/+1)$, as of left or right foot MP.

III. Frontoparietal Connections in Lower Limb MP

To demonstrate the feasibility of the proposed system, the system components were validated. The event-related potentials (ERPs) between MP and MI were visualized. As the first component of the proposed system, the classification accuracy of MP was evaluated and compared with the performance of MI. While in the second component, the evidence of the relationship between frontoparietal connectivity and classification performance was illustrated.

A. Experimental Paradigm

Eleven subjects with a mean age of 25.27($\pm$3.44) were recruited for this study. Two independent data acquisition schemes were conducted in this study, as shown in figure 2. This study was approved by the Institutional Review Board (IRB) of National Yang Ming Chiao Tung University with the case number NYCU-REC-110-011E.

1) Classification Paradigm: The first experimental scheme was conducted for two sessions. Subjects were required to perform covert motor activities, including MP and MI. Since MP precedes motor activities [38], the experiment was designed to resemble the natural motor sequence, as such that each MP cue was followed by a MI cue [33]. A trial was initiated with a fixation cue for 2 seconds, followed by a 1-second white arrow directed to the left or right. The direction of the white arrow prompted for left or right foot MP. During this period, the subjects were requested to prepare for lower limb motor movement (isometric muscle tension) without carrying out the motor movement itself. The MP paradigm was designed by referring to previous study, which the participants were told which limb to move before they were asked to move [38]. After 1 second, the color of the white arrow will be changed to either green or red. The green arrow prompted the subjects to carry on the lower limb MI (imagining motor movement), with the foot corresponding to the direction of the arrow. During this period, the subjects were instructed to perform kinesthetic MI, which is the imagination of the feeling of movements, without any real physical movement. The red arrow acted as a control measure and the subjects have to remain at rest throughout the period. Afterward, a fixation point remained on screen for 2 seconds, reminding the subjects to fix their gaze on the point. In each session, each colored (green/red) arrow was prompted exactly 50 times.

The sampling frequency of the recorded EEG signals was downsampled from the original 500 Hz to 125 Hz, and a notch filter was applied to attenuate 60 Hz power line noise. The mean impedance of the detachable gel-free Ag/AgCl electrodes was kept below 100 kΩ throughout the experiment, which falls within the reliable range to record EEG signals [39], [40], [41]. A digital bandpass filtering was performed to obtain a physiological frequency range within 8-50 Hz [42], and remove low and high-frequency artifacts. To further ameliorate overfitting due to high-dimensional connectivity features, linear SVM was selected and trained with ten-fold cross-validation (90% training data and 10% testing data). The accuracies reported in this manuscript were the

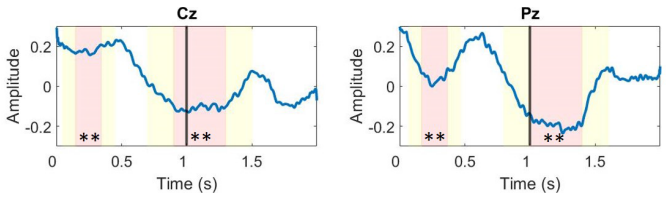

Fig. 3. The ERPs time-locked to MP and MI cues. Time 0 indicates the initiation of MP, while the black vertical lines indicate the onset of MI. The mean of windowed ERD (red) was compared with the mean amplitude of surrounding signals (yellow). Significant motor-related desynchronization was observed in both MP and MI phases (pairwise Wilcoxon signed-rank test: $**\ p < 0.01$).

testing set accuracies across ten-fold. The random threshold for two-class classification was 50%.

2) Neurofeedback Paradigm: The second experimental scheme was designed to investigate the subjective neurofeedback experience during lower limb MP/MI. The experiment was started with a 180-second resting phase, followed by six stratified left and right foot cues that lasted for 120 seconds, which were set apart by 5 second resting period. The subjects were asked to imagine lower limb movement during the 120-second imagining phase. A real-time functional connectivity-based neurofeedback was projected on the monitor during the imagining phases. The five alpha band (8-13 Hz) frontoparietal connections (P7-C4, P7-Cz, P7-FC4, P7-FCz, P7-FC3) used in this study were shown negatively related to the MI-BCI performance in the previous study [32]. The functional connections were extracted in real-time from a 1-second (downsampled to 125 Hz) time-series EEG window, bandpass filtered within 8-13 Hz. The connectivity was measured as in section II-B. The neurofeedback was presented on a computer screen, with varying shades of blue lines on a scalp image, which were inversely proportionate to the strength of five connections, as shown in figure 2. There are mainly two types of MI, which are kinesthetic imagery of movement and visual imagery of movement [43]. Subjects were given the freedom to test and perform any kind of lower limb MP/MI, including visual imagery of movement, kinesthetic imagery of movement, and isometric muscle tension or stiffness. The subjects were asked to be aware of the type of MP/MI that could produce the most significant negative (dark blue lines) frontoparietal connections. The subjects were required to discuss their experience after the neurofeedback session was completed. No classification was performed within the neurofeedback paradigm.

B. Event-Related Potential

ERPs are the average potential of time-locked EEG signals with respect to the initiation of cue [44]. Averaging EEG signals from multiple trials could eliminate random noise and increase the prominence of a task-related waveform. Since the somatosensory region of lower limbs is located at the midline of central and parietal lobes [12], the ERPs of EEG signals recorded from Cz and Pz were visualized in figure 3. Event-related desynchronization (ERD) was present around 200-400 ms after both MP and MI cues. The significance of ERDs was evaluated using the technique adopted from [45], by comparing the mean of the windowed trough (W_{ERD}) and the mean signal amplitude pre- and post-trough ERD$\pm(0.5 \times W_{ERD})$. Both ERDs after MP and MI demonstrate significant depression (pairwise Wilcoxon signed-rank test: $p < 0.01$). It was noted that the ERDs during MI were more prominent than the ERDs during MP. These results are consistent with previous studies [46], [47] which showed that MP cue evoked 200-500 ms ERD that was slightly less prominent than the ERD of motor execution [45].

C. Classification Accuracy - Static

The recorded EEG trials were truncated into a full 1-second MP phase and 1-second MI phase. Functional connectivities were extracted from each phase, as computed in equation 1. The connectivity matrices of both phases were vectorized and independently fed into linear SVM to classify left or right-foot motor intentions. Subject-specific trials were randomly partitioned into ten equal portions, where nine portions were used to train the classifier and the remaining one was used to evaluate the trained model. This process was repeated ten times until each of the ten portions was evaluated exactly once. To allow fair comparisons, no hyperparameter tuning was performed for all classifiers. The accuracy across ten folds was reported. The results in table I suggest that the left and right foot motor intentions were more distinguishable in the MP phase, compared to the MI phase (pairwise Wilcoxon signed-rank test: $p < 0.05$). Classification of left and right foot MP achieved an average accuracy of 72.18($\pm$14.42)% and 77.45($\pm$10.86)% for the first and second session respectively, while the MI phase reported accuracies of 56.91($\pm$11.15)% and 58.82($\pm$10.81)%. We further investigated the accuracy of two additional classifiers, linear discriminant analysis (LDA) and k-nearest neighbor (KNN; $k = 3$) in classifying MP and MI. Table II indicates that SVM outperformed LDA and KNN in discriminating left and right foot MP. In all three classification schemes, MP performed significantly better than MI (pairwise Wilcoxon signed-rank test: $p < 0.05$), suggesting that lower limb MP is more classifiable than MI. The classification of EEG during the post-cue fixation period was also analyzed. The lasting effect of MI was observed, where the classification accuracy gradually decreased after the disappearance of the MI cue, reporting 57.73($\pm$9.79)% and 59.45($\pm$12.16)% in the first second after the onset of fixation cue. The accuracies decreased to random guessing (47.64($\pm$8.23)% and 53.27($\pm$6.83)%) in the 1-2 seconds of post-cue fixation, suggesting that the brain activity returned to the resting state within this period. The distinguishability between MI (trials during green arrow) and rest (trials during red arrow) were 56.73($\pm$9.64)% and 64.59($\pm$8.07)% in session 1 and session 2. This showed that the functional connectivity of MI and rest were classifiable to some extent.

D. Classification Accuracy - Time-Varying

To pinpoint the frequency band and transient time window when lower limb MP/MI could be classified with the highest accuracy, a sliding window approach was implemented on the

TABLE I
CLASSIFICATION ACCURACY-STATIC

Subject	MP/MI - Left vs. Right				Post-Cue Fixation - Left vs. Right				MI (green arrow) vs. Rest (red arrow)	
	MP		MI		MP		MI		MI	
	Session 1	Session 2	Session 1	Session 2	Session 1	Session 2	Session 1	Session 2	Session 1	Session 2
1	90	84	61	75	66	63	37	54	65.5	64.5
2	79	95	65	56	57	67	49	43	65	64.5
3	56	70	53	50	45	48	51	52	55	69.5
4	73	71	69	65	60	45	45	49	66	65
5	72	79	47	61	62	65	42	52	59	62.5
6	64	69	45	44	46	48	40	43	51.5	62.5
7	72	79	54	71	62	69	36	56	45.5	48.5
8	95	90	81	68	76	82	58	62	59	73.5
9	80	64	55	62	47	56	53	52	69.5	73
10	69	63	50	42	50	67	60	64	50.5	52
11	44	88	46	53	64	44	53	59	37.5	75
Mean	**72.18**	**77.45**	56.91	58.82	57.73	59.45	47.64	53.27	56.73	64.59
Std	14.42	10.86	11.15	10.81	9.79	12.16	8.23	6.83	9.64	8.07

TABLE II
CLASSIFICATION PERFORMANCE BY THREE CLASSIFIERS-STATIC

Subject	LDA				KNN				SVM			
	MP		MI		MP		MI		MP		MI	
	Session 1	Session 2	Session 1	Session 2	Session 1	Session 2	Session 1	Session 2	Session 1	Session 2	Session 1	Session 2
1	81	69	62	74	70	61	55	61	90	84	61	75
2	76	86	54	59	78	83	51	50	79	95	65	56
3	42	70	41	46	57	72	49	51	56	70	53	50
4	69	69	59	65	59	67	57	69	73	71	69	65
5	71	72	50	46	75	61	53	53	72	79	47	61
6	51	55	51	43	65	69	44	48	64	69	45	44
7	70	62	56	66	56	64	52	63	72	79	54	71
8	95	78	66	61	85	73	55	58	95	90	81	68
9	74	65	43	57	63	64	37	55	80	64	55	62
10	50	58	52	53	58	62	38	63	69	63	50	42
11	51	83	49	67	50	79	56	47	44	88	46	53
Mean	66.36$^{\triangle}$	69.73$^{\triangle}$	53.00	57.91	65.09$^{\triangle}$	68.64$^{\triangle}$	49.73	56.18	**72.18**$^{*,\triangle}$	**77.45**$^{*,\dagger,\triangle}$	56.91†	58.82
Std	16.00	9.76	7.55	9.99	10.74	7.42	7.06	7.15	14.42	10.88	11.15	10.81

*The accuracy of SVM was significantly higher than the accuracy of LDA. (Pairwise Wilcoxon signed-rank test: $p < 0.05$).
†The accuracy of SVM was significantly higher than the accuracy of KNN. (Pairwise Wilcoxon signed-rank test: $p < 0.05$).
$^{\triangle}$The accuracy of MP was significantly higher than the accuracy of post-cue fixation. (Pairwise Wilcoxon signed-rank test: $p < 0.05$).

1-second EEG data from section III-C. The EEG signals were filtered into three main frequency ranges, which were alpha (8-13 Hz), beta (14-30 Hz), and low gamma (31-50 Hz) bands. We applied a sliding window, with a length of 200 ms (100 time points) and a stride of 20 ms (10 time points), to the filtered time-series EEG data. Functional connectivity features were extracted from each window and were trained and tested with 10-fold cross-validation. In the training phase, three SVM classifiers were independently trained with the same 90% of trials from each of the three frequency bands. The testing phase was initiated by the independent prediction of the class labels (10% testing trials) from each trained classifier. The trained classifiers were ensembled by the majority voting technique [48], [49], where the mode of predicted labels from three classifiers was determined. The mode of three predicted labels was the final predicted class of the ensemble classifier. The classification accuracy of each window was computed as the performance evaluation metrics.

We observed that all subjects exhibit varying peak classification accuracy within 200-400 ms of the MP phase, with maximum mean accuracies of 70.64(±13.94)% and 73.73(±7.99)% respectively in session 1 and session 2. This trend was consistent across three motor-related frequency bands, and thus, majority voting generated similar results. To further validate the findings, the averaged time-varying accuracy during MP/MI was compared with the accuracy during the 2-seconds fixation phase. Moreover, MP/MI signals back-projected from independent component analysis [50] (abbreviated as ICB, to distinguish from component-based signals) were also evaluated to rule out eye movement artifacts. Components prone to eye movement artifacts (Fp1, Fp2, F7, F8, FT7, FT8, T7, T8) were strictly removed. The clean components were back-projected to channel-based signals to retain consistent feature dimensions. As shown in figure 4 and table III, the accuracy trend of both filtered feature and ICB feature were similar. The accuracy trends during 200-400 ms were significantly different compared to the fixation phase (pairwise Wilcoxon signed-rank tests; $p < 0.05$). This further suggests that functional brain connectivity could distinguish left and right foot MP more efficiently than MI. However, as shown in the subject-specific results in Table III, the intra- and inter-subject variability in classification performance were present in the MP phase. For example, the peak performance of subject 2 and subject 11 varied across two experimental

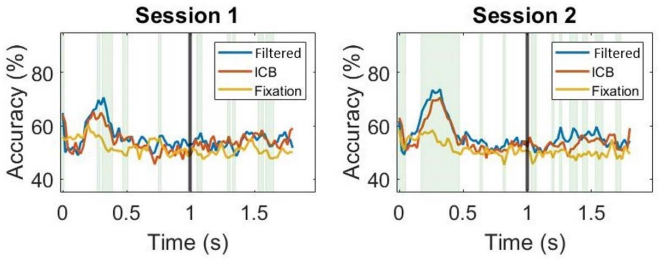

Fig. 4. Mean time-varying accuracy of session 1 and session 2. The classification accuracy of MP/MI and ICB showed significant differences with fixation (green shaded background; pairwise Wilcoxon signed-rank test: $p < 0.05$).

TABLE III
THE PEAK CLASSIFICATION ACCURACY WITHIN 200 MS - 400 MS WINDOWS

	Filtered		ICB	
Subject	Session 1	Session 2	Session 1	Session 2
1	73	67	45	54
2	76	60	75	59
3	62	67	61	64
4	79	79	65	77
5	68	67	80	65
6	65	76	64	79
7	57	69	58	69
8	99	85	79	83
9	82	81	74	74
10	70	80	65	76
11	46	80	53	76
Mean	70.64	73.73	65.36	70.55
Std	13.94	7.99	11.00	9.07

No significant different was found in accuracy between filtered and ICB features. (Pairwise Wilcoxon signed-rank test: $p > 0.01$).

sessions, while subject 7 performed comparatively poorer in both sessions.

E. Correlation Between Connectivity and Accuracy

Parietal functional connections in the range of alpha-band were found correlated to the upper limb MI-BCI performance [32]. Five frontoparietal connections (P7-C4, P7-Cz, P7-FC4, P7-FCz, P7-FC3) were extracted from each window (as in session III-D) and aligned with time-varying accuracy. Similar to the previous study [32], subjects showed decreased alpha-band connections within the 200-400 ms of MP period, which this time frame also achieved the best classification accuracy as shown in section III-D. Pearson's correlation coefficient (PCC) was computed between five connections and classification accuracy. The average correlation across subjects was tabulated in table IV. Two out of five connections (P7-C4 and P7-FC4) showed moderate negative correlation ($0.5 > |PCC| > 0.3$) with the accuracy during MP phase. On the other hand, the MI phase showed insignificant PCC between frontoparietal connectivity and accuracy. This indicates that alpha-band frontoparietal functional connectivity is correlated to the distinguishability of the lower limb during MP. We also compared the time-varying frontoparietal connectivity during the appearance of green (MP-MI) and red (MP-Rest) arrows, and during the fixation phase. As shown in figure 5, significant reduction (pairwise Wilcoxon signed-rank tests; $p < 0.05$) of frontoparietal functional connections were found in MP (in both MP-MI and MP-Rest) compared to fixation phases. The difference was more prominent around 200-400 ms of P7-FC4 connections. By comparing the connections between MP-MI and MP-Rest, significant lower frontoparietal connectivities (pairwise Wilcoxon signed-rank tests; $p < 0.05$) were found around 200-350 ms after MI cue, especially in P7-Cz and P7-FCz connections. The results suggest the difference in neural mechanisms underpinning MP and MI.

TABLE IV
CORRELATION BETWEEN ALPHA BAND FRONTOPARIETAL CONNECTIVITY AND CLASSIFICATION ACCURACY

	0 - 1 second (MP)		1 - 2 second (MI)	
Connection	Session 1	Session 2	Session 1	Session 2
P7-C4	**-0.33**	**-0.46**	0.02	0.06
P7-Cz	-0.01	-0.21	0.02	0.03
P7-FC4	**-0.47**	**-0.49**	-0.01	0.09
P7-FCz	0.02	-0.17	0.04	0.08
P7-FC3	0.24	0.25	0.04	0.08

IV. PRECLINICAL TRIALS IN POST-STROKE PATIENTS

Previous sections demonstrated the functional frontoparietal network in healthy individuals, the connectivity of post-stroke patients was further validated in this section. Since post-stroke patients experience muscle stiffness corresponding to the damaged brain area, we further investigated the alpha band functional frontoparietal connections of post-stroke patients from EEG data published in [51]. The EEG data were recorded from eight healthy subjects and nine post-stroke patients. All patients were suffering from walking difficulty due to lower limb stiffness. The subjects conducted 30 seconds of standing phase (Stand 1), followed by 60 seconds of walking phase (Walk) and another 30 seconds of standing phase (Stand 2). The EEG data were acquired through the NuAmps EEG system (Compumedics Neuroscan, Inc.) with 32 wet electrodes, at a 1 kHz sampling rate and impedance under 20 kΩ.

The comparisons were to be performed with the P7-FC4 connection, which was reported with the highest correlation in table IV. However, due to the reason that the EEG modality used did not contain P7 channels, nearby P3-FC4 connections were selected instead. The difference in P3-FC4 connection strength between healthy subjects and post-stroke patients during standing and walking phases was investigated. The intra-subject comparisons were performed with pairwise Wilcoxon signed-rank test and the inter-subject comparisons were conducted using the pairwise Mann-Whitney U test. The bar chart in figure 6 shows that post-stroke patients indeed have significantly lower P3-FC4 connections compared to healthy subjects. Furthermore, in healthy individuals, walking produced significantly stronger connections than standing. These prove that the reduction of frontoparietal connections was related to isometric muscle preparation

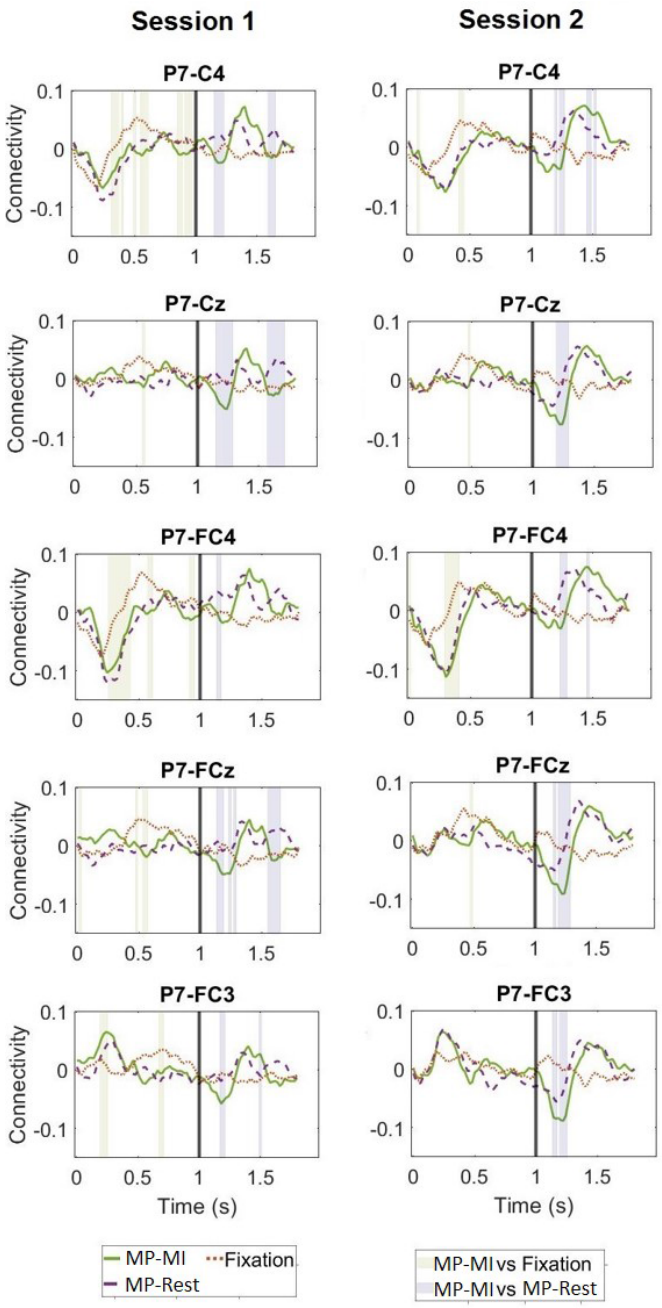

Fig. 5. Parietal connectivity in different tasks, including two MP phases (MP-MI (green) and MI-Rest (purple)) and a fixation phase (yellow). Significant differences were found during MP and fixation (green shaded areas), as well as between MP-MI and MP-Rest (purple shaded areas).

during standing, as well as the muscle stiffness in post-stroke patients. This also showed the capacity of our proposed frontoparietal-connectivity system to provide neurofeedback for the monitoring of brain recovery in the course of rehabilitation therapy.

V. Discussion

A. Lower Limb MP-BCI System

We demonstrate the feasibility of the development of the frontoparietal-connectivity-actuated lower limb MP-BCI

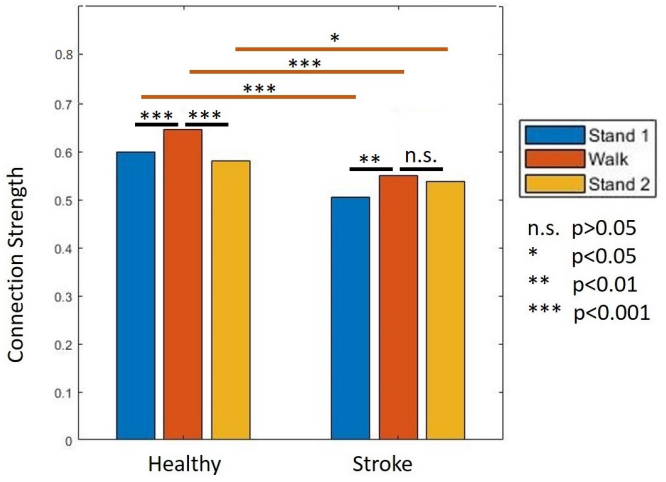

Fig. 6. Comparison of functional frontoparietal connections (P3-FC4) in healthy subjects and post-stroke patients. The intra-subject comparisons (black solid lines) were performed with pairwise Wilcoxon signed-rank test and the inter-subject comparisons (red solid lines) were conducted using pairwise Mann-Whitney U test.

system. Consistent with previous literature [46], [47], we found that MP-related potential appeared around 200-400 ms post-cue. The amplitude of MP-related potential was slightly lower than the amplitude of MI-related potential. This was the primary distinctive EEG feature between MP and MI. By classifying lower limb MP/MI, results showed that MP could achieve higher accuracy than MI. Our static classification accuracies achieved 72.18(±14.42)% and 77.45(±10.86)% in two sessions. Previous lower limb MI studies reported classification accuracy of 63.0%, 69.3%, and 83.82% by using EEG frequency power [52], beta rebound [16], and the combination of intrinsic time-scale decomposition and artificial neural networks [53], respectively. Although our results showed accuracy lower than [53], our proposed model implemented by SVM carries a relatively lower computational cost than artificial neural network. This could facilitate the usage of the lower-limb BCI system in a real-world setting.

The peak of accuracy was prominent around 200-400 ms post-cue, which was in sync with MP-related potential. This short-lived performance peak in MI was also observed in [54], which they reported an accuracy peak of 80.0% - 83.6%. This suggests the feasibility to classify motor-related brain activity by transient EEG signatures. However, since MP/MI/ME are continuous sequential processes [38], we could not infer the benefit of reducing the trial time of motor-based BCI. Future study will be carried out to investigate and compare the performance of different MP/MI periods. The peak performance found in our study was moderately correlated to the negativity of left parietal and right frontocentral connections (P7-FC4 and P7-C4). Published literature had investigated the inter-subjects relationship between BCI performance and EEG features, such as power spectral density of C3 and C4 [29], [55], theta activity of frontal lobe [56], gamma activity of frontal and central cortices [57], and frontoparietal resting network [58]. Our study emphasized on intra-subjects variability demonstrates the decrement of functional frontoparietal connectivity during

MP was correlated to the increment of lower limb classification accuracy.

B. SVM Features Weights

The weights of linear SVM trained to classify broadband (8-50 Hz) left and right foot MP functional connectivity were extracted to investigate the most distinguishing features. To equally analyze the feature importance, the linear SVM was trained with all MP trials and the feature weights were ranked. From each subject, the top ten weighted features were selected for comparison purpose. We tabulated these connections based on the connections between different brain areas, namely frontal (F), central (C), parietal (P), temporal (T), and occipital (O) regions. The quantitative summary in table V is the total number of top ten weighted connections between predefined brain areas. The results suggested that frontocentral (24) connections contributed the most to the classification of left and right foot MP, followed by frontotemporal (15), centrocentral (12), and parietotemporal (11) connections. The reported features were consistent with previous lower limb MI study [28]. Central motor cortices were long found to contribute to motor activity [12]. Anterior prefrontal regions were also proposed to be involved in decision-making during the preparation of foot movement [59]. Motor planning was found accompanied by the activation of the parietal cortex [60], [61]; while the temporal lobe was hypothesized to be related to the learning of performing MI [28]. Our results show that the integration of functional connections from different brain areas could distinguish lower limb MP better than MI. However, the performance of classifying lower limb MP was not generalized within and across subjects. Future study could implement transfer learning techniques [62] such as deep learning-based adversarial variational autoencoders [63] to improve the generalizability of MP-based BCI.

TABLE V
QUANTITATIVE REPRESENTATION OF TOP TEN WEIGHTED CONNECTIONS BETWEEN PREDEFINED BRAIN AREAS

	Subject											
Connection	1	2	3	4	5	6	7	8	9	10	11	Total
F-C	1	4	2	1	0	5	1	2	2	2	4	24
F-P	2	0	1	1	0	0	1	0	0	2	1	8
F-O	0	0	0	0	0	0	0	0	0	0	0	0
F-T	3	0	0	1	2	1	0	4	0	1	3	15
C-P	0	0	0	1	1	1	2	0	2	0	0	7
C-O	1	0	0	0	0	0	0	0	1	0	0	2
P-O	1	3	1	0	2	0	0	0	0	1	0	8
C-T	0	0	0	2	1	0	1	1	2	0	0	7
P-T	0	2	0	2	1	1	1	1	2	0	1	11
O-T	0	0	0	0	0	1	1	0	0	0	0	2
F-F	0	0	1	1	0	0	1	1	0	0	1	5
C-C	0	1	4	0	2	1	0	1	1	2	0	12
P-P	1	0	1	1	1	0	1	0	0	1	0	6
O-O	1	0	0	0	0	0	0	0	0	0	0	1
T-T	0	0	0	0	0	0	1	0	0	1	0	2

F: frontal; C: central; P: parietal; T: temporal; O: occipital.

C. Subjective Experience of Functional Frontoparietal Connections

This section elaborates on the subjective experience during connectivity-based neurofeedback. As written in section III-A.2, real-time alpha band frontoparietal connectivities were projected on a computer screen when the subjects were performing MI. In this experimental paradigm, subjects were given the freedom to test and perform any kind of lower limb MP/MI, and report the type of MP/MI that they found could produce the most negative frontoparietal connections. Nine out of eleven (81.82%) subjects revealed that the negativity of frontoparietal connections was increased when they perform MP, including the isometric muscle strain, muscle tension, and muscle stiffness. The remaining two subjects (18.18%) informed that attention increased the negativity of their functional frontoparietal connections. These results propose that the muscle strain during MP could be related to the negativity of functional frontoparietal connections within the range of the alpha band.

Existing human study based on positron emission tomography has visualized that frontal and parietal lobes were activated during MP [64]. High-level motor behaviors such as motor planning, the formation of motor intention, and sensory-motor integration were correlated to the activity of the parietal cortex [60]. The dorsal premotor cortex (PMd) located at the lateral prefrontal cortex was also found involved in MP [65]. Transient frontoparietal activation was also found around 300-450 ms of motor intention [66]. These findings are consistent with our results which frontoparietal and centroparietal connections (P7-FC4 and P7-C4) are transiently correlated ($|PCC| = 0.49$ and 0.47) to MP. Additional EEG analysis from healthy subjects and post-stroke patients further support the neuromechanism between isometric muscle strain and the negativity of frontoparietal connection (the functional connectivity changes in post-stroke patients were reviewed in [67]). This suggests the potential development of a frontoparietal-connectivity-based neurofeedback system to evaluate the recovery outcome of the central nervous system during rehabilitation training.

VI. CONCLUSION

We proposed a wearable frontoparietal-connectivity-actuated lower limb MP-BCI system for the detection of bipedal lower limb MP. We found that the lower limb MP could achieve significantly better accuracy in classifying left and right foot, compared to the motor imagery. Frontocentral, frontotemporal, centrocentral, and parietotemporal connections were found to contribute the most to the distinguishability of left and right foot MP. The peak classification accuracy was around 200-400 ms of the MP phase, which was accompanied by the reduction of P7-FC4 and P7-C4 connectivity strength in the alpha range. The decrease in connectivity strength was suggested to be related to the isometric muscle preparation. These results validated the utilization of the motor preparation with reduced frontoparietal connectivity to achieve better performance in discriminating left and right foot brain activities. In future study, MP-BCI users could be trained to modulate their alpha band frontoparietal connectivity to

improve BCI efficacy. Furthermore, a similar neurofeedback paradigm could be also implemented to monitor motor-related brain activity during post-stroke rehabilitation training. One of the limitations of this study is the lack of system validation on post-stroke patients. In the future, we will perform clinical trials to evaluate the performance of the proposed system during rehabilitation training, and analyze the relationship between the frontoparietal connectivity and muscle stiffness in post-stroke patients. Moreover, the study could extend the current synchronous system to an asynchronous BCI system to provide a more natural MP/MI paradigm.

REFERENCES

[1] Y. Liu, Z. Li, T. Zhang, and S. Zhao, "Brain–robot interface-based navigation control of a mobile robot in corridor environments," *IEEE Trans. Syst., Man, Cybern., Syst.*, vol. 50, no. 8, pp. 3047–3058, Aug. 2020.

[2] J. Meng and B. He, "Exploring training effect in 42 human subjects using a non-invasive sensorimotor rhythm based online BCI," *Frontiers Hum. Neurosci.*, vol. 13, p. 128, Apr. 2019.

[3] A. Frolov et al., "Preliminary results of a controlled study of BCI–exoskeleton technology efficacy in patients with poststroke arm paresis," *Bull. Russian State Med. Univ.*, vol. 2, pp. 16–23, Mar. 2016.

[4] T. Carlson and J. Del R Millan, "Brain-controlled wheelchairs: A robotic architecture," *IEEE Robot. Autom. Mag.*, vol. 20, no. 1, pp. 65–73, Mar. 2013.

[5] S. He et al., "EEG- and EOG-based asynchronous hybrid BCI: A system integrating a speller, a web browser, an E-mail client, and a file explorer," *IEEE Trans. Neural Syst. Rehabil. Eng.*, vol. 28, no. 2, pp. 519–530, Feb. 2020.

[6] H. Cecotti, "Adaptive time segment analysis for steady-state visual evoked potential based brain–computer interfaces," *IEEE Trans. Neural Syst. Rehabil. Eng.*, vol. 28, no. 3, pp. 552–560, Mar. 2020.

[7] J. Jin et al., "The study of generic model set for reducing calibration time in P300-based brain–computer interface," *IEEE Trans. Neural Syst. Rehabil. Eng.*, vol. 28, no. 1, pp. 3–12, Jan. 2020.

[8] L. F. Nicolas-Alonso and J. Gomez-Gil, "Brain computer interfaces, a review," *Sensors*, vol. 12, no. 2, pp. 1211–1279, 2012.

[9] A. Jiang, J. Shang, X. Liu, Y. Tang, H. K. Kwan, and Y. Zhu, "Efficient CSP algorithm with spatio-temporal filtering for motor imagery classification," *IEEE Trans. Neural Syst. Rehabil. Eng.*, vol. 28, no. 4, pp. 1006–1016, Apr. 2020.

[10] P. Wierzgała, D. Zapała, G. M. Wojcik, and J. Masiak, "Most popular signal processing methods in motor-imagery BCI: A review and meta-analysis," *Frontiers Neuroinform.*, vol. 12, pp. 1–10, Nov. 2018.

[11] L.-W. Ko et al., "Multimodal fuzzy fusion for enhancing the motor-imagery-based brain computer interface," *IEEE Comput. Intell. Mag.*, vol. 14, no. 1, pp. 96–106, Feb. 2019.

[12] A. S. F. Leyton and C. S. Sherrington, "Observations on the excitable cortex of the chimpanzee, orang-utan, and gorilla," *Quart. J. Experim. Physiol.*, vol. 11, no. 2, pp. 135–222, Jul. 1917.

[13] C. Stippich, H. Ochmann, and K. Sartor, "Somatotopic mapping of the human primary sensorimotor cortex during motor imagery and motor execution by functional magnetic resonance imaging," *Neurosci. Lett.*, vol. 331, no. 1, pp. 50–54, 2002. [Online]. Available: http://www.ncbi.nlm.nih.gov/pubmed/12359321

[14] A. M. Batula, J. A. Mark, Y. E. Kim, and H. Ayaz, "Comparison of brain activation during motor imagery and motor movement using fNIRS," *Comput. Intell. Neurosci.*, vol. 2017, pp. 1–12, Mar. 2017.

[15] M. Sun, H. Akiyoshi, T. Igasaki, and N. Murayama, "Asynchronous brain-computer interface with foot motor imagery," in *Proc. Int. Conf. Complex Med. Eng. (ICME)*, May 2013, pp. 191–196.

[16] Y. Hashimoto and J. Ushiba, "EEG-based classification of imaginary left and right foot movements using beta rebound," *Clin. Neurophysiol.*, vol. 124, no. 11, pp. 2153–2160, Nov. 2013, doi: 10.1016/j.clinph.2013.05.006.

[17] C.-R. Phang, F. Noman, H. Hussain, C.-M. Ting, and H. Ombao, "A multi-domain connectome convolutional neural network for identifying schizophrenia from EEG connectivity patterns," *IEEE J. Biomed. Health Informat.*, vol. 24, no. 5, pp. 1333–1343, May 2020.

[18] F. Liu et al., "Dynamic functional network connectivity in idiopathic generalized epilepsy with generalized tonic–clonic seizure," *Hum. Brain Mapping*, vol. 38, no. 2, pp. 957–973, 2017.

[19] D. J. Englot et al., "Relating structural and functional brainstem connectivity to disease measures in epilepsy," *Neurology*, vol. 91, no. 1, pp. e67–e77, 2018.

[20] D. H. Hepp, E. M. J. Foncke, K. T. E. Olde Dubbelink, W. D. J. van de Berg, H. W. Berendse, and M. M. Schoonheim, "Loss of functional connectivity in patients with Parkinson disease and visual hallucinations," *Radiology*, vol. 285, no. 3, pp. 896–903, Dec. 2017.

[21] G.-J. Ji et al., "Functional connectivity of the corticobasal ganglia–thalamocortical network in Parkinson disease: A systematic review and meta-analysis with cross-validation," *Radiology*, vol. 287, no. 3, pp. 973–982, 2018.

[22] J. King et al., "Increased functional connectivity after listening to favored music in adults with Alzheimer dementia," *J. Prevention Alzheimer's Disease*, vol. 6, no. 1, pp. 56–62, 2019.

[23] A. Mohan et al., "The significance of the default mode network (DMN) in neurological and neuropsychiatric disorders: A review," *Yale J. Biol. Med.*, vol. 89, no. 1, pp. 49–57, 2016.

[24] A. Anand, "Functional and structural connectome in mood disorders mood disorders: Clinical applications," *Frontiers Psychiatry*, vol. 10, p. 202, Mar. 2019.

[25] K. Rubia et al., "Functional connectivity changes associated with fMRI neurofeedback of right inferior frontal cortex in adolescents with ADHD," *NeuroImage*, vol. 188, pp. 43–58, Mar. 2019.

[26] M. Hamedi, S. H. Salleh, and A. M. Noor, "Electroencephalographic motor imagery brain connectivity analysis for BCI: A review," *Neural Comput.*, vol. 28, no. 6, pp. 999–1041, Jun. 2016.

[27] L. Brusini, F. Stival, F. Setti, E. Menegatti, G. Menegaz, and S. F. Storti, "A systematic review on motor-imagery brain-connectivity-based computer interfaces," *IEEE Trans. Human-Mach. Syst.*, vol. 51, no. 6, pp. 725–733, Dec. 2021.

[28] C.-R. Phang and L.-W. Ko, "Global cortical network distinguishes motor imagination of the left and right foot," *IEEE Access*, vol. 8, pp. 103734–103745, 2020.

[29] B. Blankertz et al., "Neurophysiological predictor of SMR-based BCI performance," *NeuroImage*, vol. 51, no. 4, pp. 1303–1309, 2010.

[30] C. Vidaurre and B. Blankertz, "Towards a cure for BCI illiteracy," *Brain Topogr.*, vol. 23, no. 2, pp. 194–198, Jun. 2010.

[31] J.-G. Yoon and M. Lee, "Effective correlates of motor imagery performance based on default mode network in resting-state," in *Proc. 8th Int. Winter Conf. Brain-Comput. Interface (BCI)*, Feb. 2020, pp. 1–5.

[32] C.-R. Phang and L.-W. Ko, "Intralobular and interlobular parietal functional network correlated to MI-BCI performance," *IEEE Trans. Neural Syst. Rehabil. Eng.*, vol. 28, no. 12, pp. 2671–2680, Dec. 2020.

[33] V. Morash, O. Bai, S. Furlani, P. Lin, and M. Hallett, "Classifying EEG signals preceding right hand, left hand, tongue, and right foot movements and motor imageries," *Clin. Neurophysiol.*, vol. 119, pp. 2570–2578, Nov. 2008.

[34] N. Mammone, C. Ieracitano, and F. C. Morabito, "A deep CNN approach to decode motor preparation of upper limbs from time–frequency maps of EEG signals at source level," *Neural Netw.*, vol. 124, pp. 357–372, Apr. 2020.

[35] *Artise Biomedical*. Accessed: Aug. 13, 2021. [Online]. Available: https://www.artisebio.com/

[36] C. He, R. K. Chikara, C.-L. Yeh, and L.-W. Ko, "Neural dynamics of target detection via wireless EEG in embodied cognition," *Sensors*, vol. 21, no. 15, p. 5213, Jul. 2021.

[37] C. Cortes and V. Vapnik, "Support-vector networks," *Mach. Learn.*, vol. 20, no. 3, pp. 273–297, Jul. 1995.

[38] K. C. Ames, S. I. Ryu, and K. V. Shenoy, "Simultaneous motor preparation and execution in a last-moment reach correction task," *Nature Commun.*, vol. 10, no. 1, pp. 1–13, Dec. 2019.

[39] H. Hinrichs, M. Scholz, A. K. Baum, J. W. Y. Kam, R. T. Knight, and H.-J. Heinze, "Comparison between a wireless dry electrode EEG system with a conventional wired wet electrode EEG system for clinical applications," *Sci. Rep.*, vol. 10, no. 1, pp. 1–14, Dec. 2020.

[40] Y. Higashi, Y. Yokota, and Y. Naruse, "Signal correlation between wet and original dry electrodes in electroencephalogram according to the contact impedance of dry electrodes," in *Proc. 39th Annu. Int. Conf. IEEE Eng. Med. Biol. Soc. (EMBC)*, Jul. 2017, pp. 1062–1065.

[41] T. C. Ferree, P. Luu, G. S. Russell, and D. M. Tucker, "Scalp electrode impedance, infection risk, and EEG data quality," *Clin. Neurophysiol.*, vol. 112, no. 3, pp. 536–544, 2001.

[42] M. Mirnaziri, M. Rahimi, S. Alavikakhaki, and R. Ebrahimpour, "Using combination of μ, β and γ bands in classification of EEG signals," *Basic Clin. Neurosci.*, vol. 4, no. 1, pp. 76–87, 2013.
[43] C. Schuster et al., "Best practice for motor imagery: A systematic literature review on motor imagery training elements in five different disciplines," *BMC Med.*, vol. 9, no. 1, pp. 1–35, 2011.
[44] S. J. Luck, *An Introduction to the Event-Related Potential Technique*. Cambridge, MA, USA: MIT Press, 2014.
[45] M. Zaepffel, R. Trachel, B. E. Kilavik, and T. Brochier, "Modulations of EEG beta power during planning and execution of grasping movements," *PLoS ONE*, vol. 8, no. 3, Mar. 2013, Art. no. e60060.
[46] Y. Wang and S. Makeig, "Predicting intended movement direction using EEG from human posterior parietal cortex," in *Proc. Int. Conf. Found. Augmented Cognition*. Berlin, Germany: Springer, 2009, pp. 437–446.
[47] M.-P. Deiber, E. Sallard, C. Ludwig, C. Ghezzi, J. Barral, and V. Ibañez, "EEG alpha activity reflects motor preparation rather than the mode of action selection," *Frontiers Integrative Neurosci.*, vol. 6, p. 59, Mar. 2012.
[48] K. Belwafi, S. Gannouni, H. Aboalsamh, H. Mathkour, and A. Belghith, "A dynamic and self-adaptive classification algorithm for motor imagery EEG signals," *J. Neurosci. Methods*, vol. 327, Nov. 2019, Art. no. 108346.
[49] R. Chatterjee, A. Datta, and D. K. Sanyal, "Ensemble learning approach to motor imagery EEG signal classification," in *Machine Learning in Bio-Signal Analysis and Diagnostic Imaging*. Amsterdam, The Netherlands: Elsevier, 2019, pp. 183–208.
[50] T.-P. Jung et al., "Removing electroencephalographic artifacts by blind source separation," *Psychophysiology*, vol. 37, no. 2, pp. 163–178, 2000.
[51] L.-W. Ko et al., "Integrated gait triggered mixed reality and neurophysiological monitoring as a framework for next-generation ambulatory stroke rehabilitation," *IEEE Trans. Neural Syst. Rehabil. Eng.*, vol. 29, pp. 2435–2444, 2021.
[52] A. Kline, C. Gaina Ghiroaga, D. Pittman, B. Goodyear, and J. Ronsky, "EEG differentiates left and right imagined lower limb movement," *Gait Posture*, vol. 84, pp. 148–154, Feb. 2021.
[53] E. A. Mohamed, M. Z. Yusoff, A. S. Malik, M. R. Bahloul, D. M. Adam, and I. K. Adam, "Comparison of EEG signal decomposition methods in classification of motor-imagery BCI," *Multimedia Tools Appl.*, vol. 77, no. 16, pp. 21305–21327, 2018.
[54] G. Pfurtscheller, R. Scherer, G. R. Müller-Putz, and F. H. Lopes da Silva, "Short-lived brain state after cued motor imagery in naive subjects," *Eur. J. Neurosci.*, vol. 28, no. 7, pp. 1419–1426, Oct. 2008.
[55] C. Sannelli, C. Vidaurre, K.-R. Müller, and B. Blankertz, "A large scale screening study with a SMR-based BCI: Categorization of BCI users and differences in their SMR activity," *PLoS ONE*, vol. 14, no. 1, Jan. 2019, Art. no. e0207351.
[56] M. Ahn, H. Cho, S. Ahn, and S. C. Jun, "High theta and low alpha powers may be indicative of BCI-illiteracy in motor imagery," *PLoS ONE*, vol. 8, no. 11, Nov. 2013, Art. no. e80886.
[57] M. Grosse-Wentrup, B. Schölkopf, and J. Hill, "Causal influence of gamma oscillations on the sensorimotor rhythm," *NeuroImage*, vol. 56, no. 2, pp. 837–842, May 2011.
[58] T. Zhang et al., "Structural and functional correlates of motor imagery BCI performance: Insights from the patterns of fronto-parietal attention network," *NeuroImage*, vol. 134, pp. 475–485, Jul. 2016.
[59] C. Sahyoun, A. Floyer-Lea, H. Johansen-Berg, and P. M. Matthews, "Towards an understanding of gait control: Brain activation during the anticipation, preparation and execution of foot movements," *NeuroImage*, vol. 21, no. 2, pp. 568–575, Feb. 2004.
[60] R. A. Andersen and C. A. Buneo, "Intentional maps in posterior parietal cortex," *Annu. Rev. Neurosci.*, vol. 25, no. 1, pp. 189–220, Mar. 2002.
[61] J. C. Culham, C. Cavina-Pratesi, and A. Singhal, "The role of parietal cortex in visuomotor control: What have we learned from neuroimaging?" *Neuropsychologia*, vol. 44, no. 13, pp. 2668–2684, Jan. 2006.
[62] P. Wang, J. Lu, B. Zhang, and Z. Tang, "A review on transfer learning for brain-computer interface classification," in *Proc. 5th Int. Conf. Inf. Sci. Technol. (ICIST)*, Apr. 2015, pp. 315–322.
[63] O. Ozdenizci, Y. Wang, T. Koike-Akino, and D. Erdogmus, "Transfer learning in brain-computer interfaces with adversarial variational autoencoders," 2018, *arXiv:1812.06857*.
[64] M. P. Deiber, V. Ibanez, N. Sadato, and M. Hallett, "Cerebral structures participating in motor preparation in humans: A positron emission tomography study," *J. Neurophysiol.*, vol. 75, no. 1, pp. 233–247, Jan. 1996.
[65] S. R. Simon, M. Meunier, L. Piettre, A. M. Berardi, C. M. Segebarth, and D. Boussaoud, "Spatial attention and memory versus motor preparation: Premotor cortex involvement as revealed by fMRI," *J. Neurophysiol.*, vol. 88, no. 4, pp. 2047–2057, Oct. 2002.
[66] P. Praamstra, L. Boutsen, and G. W. Humphreys, "Frontoparietal control of spatial attention and motor intention in human EEG," *J. Neurophysiol.*, vol. 94, no. 1, pp. 764–774, Jul. 2005.
[67] A. G. Guggisberg, P. J. Koch, F. C. Hummel, and C. M. Buetefisch, "Brain networks and their relevance for stroke rehabilitation," *Clin. Neurophysiol.*, vol. 130, no. 7, pp. 1098–1124, Jul. 2019.